(Received 31 October 2023, Accepted 26 December 2023, Scheduled 2 January 2024)

Flux Weakening Control and Experimental Verification of Hybrid Excitation Field Modulation Synchronous Machine for Direct Drive Propulsion

Jiming Luo[1], Yang Zhang[1, 2, *], Enzhao Lu[1], Quanzhen Huang[1, 2], Mingming Huang[1], and Duane Decker[3]

[1] *School of Electrical Information Engineering, Henan University of Engineering, Zhengzhou 451191, China*
[2] *Power Integration and Intelligent Control Center, Industrial Software Industry Research Institute, Henan University of Engineering, Zhengzhou 451191, China*
[3] *School of FOCUS Engineering, Portland State University, Portland, P.O. Box 751, USA*

ABSTRACT: With combining the advantages of the hybrid excited machine and field modulation machine, hybrid excitation field modulation machine (HEFMM) exhibits obvious merits of controllable flux operation and independent flux distribution paths, which is one promising candidate for direct drive application fields. As one newly branch of hybrid excitation synchronous machine (HESM), HEFMM control method can be executed based on the characteristics of the machine operating in different speed regions. When it operates in the low-speed constant power region, the minimum copper loss method is used to optimize the *d*-axis, *q*-axis, and excitation current values. When it operates in the high-speed constant power characteristic region, flux weakening fuzzy control strategy combined with particle swarm optimization algorithm for HEFMM was presented. The correctness and effectiveness of the proposed flux weakening fuzzy control strategy were verified by the simulation data and experimental results, which demonstrated that the this current optimization method based on PSO algorithm can effectively reduce the total copper loss of the machine by 22.8%, the range of speed regulation with higher efficiency are obtained.

1. INTRODUCTION

Compared with conventional permanent magnet synchronous machine (PMSM) and reluctance machine for the application of industrial fields [1–3], hybrid excitation synchronous machine (HESM) is one promising candidate due to the feature of wide range speed regulation operation by adjusting the excitation current and d-axis current, especially for wind power generation, electric vehicles (EVs), hybrid EVs and other direct drive systems [4–7]. In recent years, several different potential solutions of HESMs exhibiting the field modulation topology [8–12], namely, hybrid excitation field modulation machine (HEFMM), has been become the key research subject since it incorporates the merits of HESM and unique magnetic field modulation principle.

In order to increase the speed range of the machine, a hybrid excitation field modulation machine was proposed with variable magnetic flux in [13], which is based on the multi-tooth split pole magnetic field modulation machine. The excitation winding and armature winding are arranged between the stator cavity gaps to achieve controllable magnetic flux. In [14], two types of flux memory magnetic field modulation motors with different rotor permanent magnet and stator permanent magnet types were proposed. This type of memory magnetic field modulation motor utilizes the high remanence and low coercivity characteristics of aluminum nickel cobalt permanent magnet material to achieve online magnetization adjustment by applying charging and demagnetizing currents, suitable for wide speed electric vehicles and ship propulsion. One pair of series and parallel HESMs having similar topologies and PM cost are assessed and compared to differentiate their advantages and disadvantages based on the partitioned stator platform in [15]. And their prototypes are fabricated and tested to validate the analyses of the flux regulation, energy conversion capability, parasitic effects and irreversible demagnetization of the two kinds of proposed machines. A new kind of AC-excited hybrid HESM is studied in [16], and three different flux-weakening control strategies are compared and investigated, respectively. All those control methods can widen the operating region of the machine to a certain extent, and do not depend on its parameters. Three models of 40 kW HESMs are proposed for the electric vehicle application in [17], which are based on auxiliary to main field excitation ratios. With the purpose of investigating the effect of hybridization ratio on the machine performance, a comparison research is implemented at rated speed, low-speed region or maximum torque per ample region, and high-speed region or field weakening region.

In [18], the machine flux-weakening implement is realized by imposing on the stator armature winding and rotor excitation winding currents, which means stator armature current control with a proper linearization voltage loop and rotor excitation current control with the purpose of enlarging operation speed by feed-forward method are designed, respectively. In [19], a local minimum function control method for the instantaneous value of reverse energy based on the dynamic characteristics

* Corresponding author: Yang Zhang (yangzhang@haue.edu.cn).

of the HESM at twice the nominal speed is presented. This method does not need to modify the controller parameters every time, and its validation is obtained in four different structures of HESMs. Similar novel HESM drive control methods with $i_d = 0$ and flux-weakening strategy, are proposed in [20] and [21], respectively. With the purpose of improving the control system robustness capacity, proportional-integral (PI) controller parameters are optimized by particle swarm optimization (PSO) algorithm. Prototype test results indicate that the PSO-PI controller is effective to reduce the torque ripple. In addition, one novel hybrid excitation field modulation machine is presented and analyzed in [22], which contains DC-biased sinusoidal phase current, and its optimal current control configurations are studied systematically. These research achievements have positive reference for revealing the electromagnetic characteristics of HEFMM. However, as a newly branch of HESM, HEFMM has been proven to be a multivariable nonlinear high-order system with strong coupling, and its electromagnetic torque is jointly related to d-axis, q-axis and excitation currents. However, the influence of power supply voltage was not taken into account in the weak magnetic control process, which means that the weak magnetic field of the d-axis current was not utilized. For HEFMM, due to the nonlinear characteristics between torque and current, different combinations of armature and excitation current may produce the same torque value, which means that the corresponding losses and rated voltage depend on the relevant current, respectively. Therefore, within the entire working range of low speed constant torque and high speed constant power, how to reduce total loss by allocating reasonable current to achieve the goal of improving the efficiency of HEFMM drive system.

This paper is organized as follows. The topology and its mathematical model of the proposed HEFMM are demonstrated in Section 2. Then, the proposed HEFMM flux weakening control strategy is described and derived in Section 3, which includes two parts of minimum copper loss (MCL) control in low speed operating area and weakening flux fuzzy control combining with PSO algorithm for high speed operating area, respectively. The control system simulation model for the proposed HEFMM is established, simulated and analyzed in Section 4. Several experimental verifications under different motion conditions for the HEFMM are given in Section 5, respectively.

2. TOPOLOGY AND MATHEMATIC MODEL OF HEFMM

Figure 1 shows the proposed three-phase HEFMM. The stator part of the machine forms a circumferential distribution of small teeth by adding the traditional permanent magnet motor tooth boots to deeper auxiliary grooves in the tooth boot parts. These teeth act as the magnetic rings in the magnetic gears, that is, the flux modulation poles. The three-phase centralized armature windings are nested on the inner stator teeth, and the DC excitation windings are evenly distributed between the adjacent flux modulation poles (FMPS) and stator teeth. The air gap flux distribution of HEFMM is composed of two components, one is constant flux created by PM, and the other is variable flux generated by field winding. The magnetic field generated by the excitation current are mostly entered into the air gap through the core because the magnetic resistance of PM is much larger than that of the core. Hence, when the machine works in flux-weakening, the permanent demagnetization for rotor PM can be avoided. Meanwhile, a satisfactory magnetic flux adjusting capacity can be obtained by regulating the currents of excitation and the d-axis due to the small reluctance of the whole magnetic circuit. For the proposed HEFMM, there are nine stator teeth and eighteen FPMs are evenly distributed upon the entire machine, respectively, and each stator tooth contains two FMPs. According to the principle of magnetic gear effect, the transmission ratio for the proposed HEFMM is 4.5. This means that the magnetic field of the inner stator armature winding changes at a rate 4.5 times the outer rotor rotation rate, allowing the inner stator armature magnetic field to rotate at a rate of increase that is a multiple of the HEFMM's transmission ratio. For every one-degree change in the rotation of the outer rotor, the magnetic field of the inner stator changes by 4.5 degrees, which means that a very small change in the position of the outer rotor will bring about a large change in the magnetic field of the stator, thus realizing the magnetic field modulation effect.

It can also be found that the magnetic field component generated by the DC excitation current is coupled with that of stator armature current and PMs from Fig. 1(b). The air gap magnetic field distribution of the proposed HEFMM is the result of the combined effect of the PMs, DC excitation windings, and the linear superposition of the stator armature windings. Therefore, the motor air gap magnetic field adjustment can be accomplished by changing the direction and size of the DC excitation current and the machine d-axis current to realize the purpose of widening the motor speed regulation range. HEFMM equivalent circuit model is shown in Fig. 2.

According to the d-q coordinate system of HEFMM, voltage, flux linkage and electromagnetic torque equations for HEFMM can be derived as follows:

Voltage equation can be expressed as:

$$\begin{bmatrix} u_f \\ u_d \\ u_q \end{bmatrix} = \begin{bmatrix} sM_{sf} & 0 & R_f + sL_f \\ R_s + sL_d & -\omega_e L_q & sM_{sf} \\ \omega_e L_d & R_s + sL_q & \omega_e M_{sf} \end{bmatrix} \begin{bmatrix} i_f \\ i_d \\ i_q \end{bmatrix} + \begin{bmatrix} 0 \\ 0 \\ \omega_e \psi_{pm} \end{bmatrix} \quad (1)$$

where u_f, u_d, and u_q are the excitation voltage, d- and q-axis armature voltage components, respectively; R_s and R_f are the stator armature and excitation winding resistance, respectively; M_{sf} is the mutual inductance between the stator armature and the excitation windings; L_d, L_q and L_f are the d-axis, q-axis and excitation inductance components, respectively; ω_e is the HEFMM electrical angular velocity; i_f, i_d and i_q are excitation current, d- and q-axis current components, respectively; ψ_{pm} is the PM flux linkage.

HEFMM flux linkage equation can be expressed as

$$\begin{bmatrix} \psi_d \\ \psi_q \end{bmatrix} = \begin{bmatrix} L_d & 0 & M_{sf} \\ 0 & L_q & 0 \end{bmatrix} \begin{bmatrix} i_d \\ i_q \\ i_f \end{bmatrix} + \begin{bmatrix} \psi_{pm} \\ 0 \end{bmatrix} \quad (2)$$

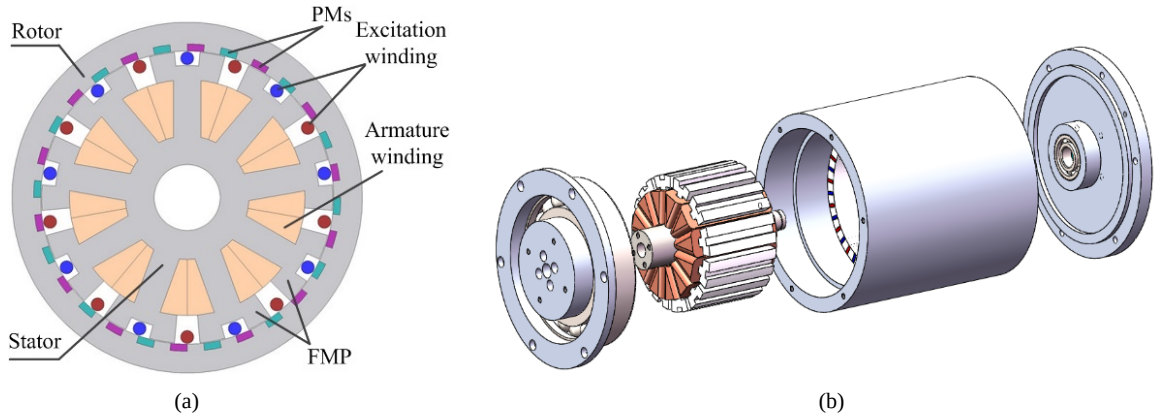

FIGURE 1. Proposed HEFMM. (a) Machine topology. (b) Exploded view.

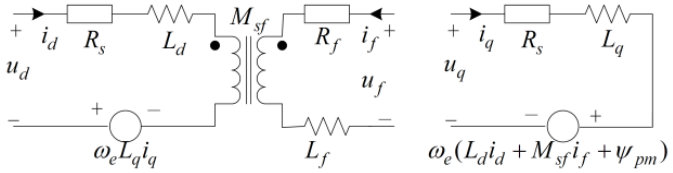

FIGURE 2. Equivalent circuits of HEFMM.

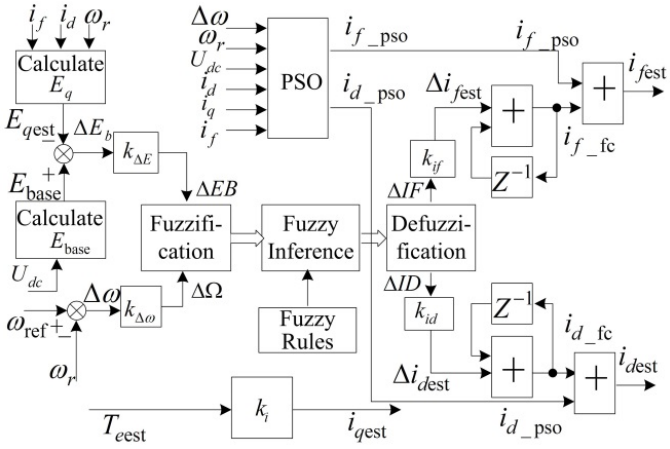

FIGURE 3. The block diagram of incremental fuzzy control combining with PSO algorithm.

where ψ_d and ψ_q are the HEFMM d- and q-axis flux linkages, respectively; where T_e is the electromagnetic torque of HEFMM; p is the number of pole pairs of the HEFMM.

The d-axis flux linkage of HEFMM generates by stator armature magnetic field current, PM and d-axis current together, as shown in (2). It is worth noting that the value of the flux linkage for PMs can be considered constant. Hence, holding d-axis flux linkage invariant, the relationship between the field current and d-axis current variations can be obtained by

$$\Delta i_f = -\frac{\Delta i_d L_d}{M_{sf}} \tag{3}$$

HEFMM electromagnetic torque equation can be expressed as

$$\begin{aligned} T_e &= J_m \frac{d\omega}{dt} + T_L + \lambda\omega \\ &= \frac{3}{2} p i_q \left[\psi_{pm} + i_d(L_d - L_q) + M_{sf} i_f\right] \end{aligned} \tag{4}$$

The total HEFMM copper loss can be expressed as

$$P_{cu} = \frac{3}{2} R_s \left(i_d^2 + i_q^2\right) + R_f i_f^2 \tag{5}$$

It can be found that the HEFMM efficiency can be enhanced by reducing the total copper loss P_{cu}. More specifically, i_d, i_q, and i_f are replaced by the estimated values of i_{dest} in the d-axis, i_{qest} in the q-axis, and i_{fest} in the field currents, respectively, and the actual torque T_e is replaced by the estimated torque T_{eest}, which is optimized based on the Lagrangian optimization theory with Lagrange multiplier, and the Lagrangian functional equation is expressed as follows

$$\begin{aligned} L(i_{dest}, i_{qest}, i_{fest}, \lambda) &= \frac{3}{2} R_s \left(i_{dest}^2 + i_{qest}^2\right) + R_f i_{fest}^2 \\ &+\lambda \left\{ \frac{3}{2} p i_{qest} \left[\psi_{pm} + i_{dest}(L_d - L_q) + M_{sf} i_{fest}\right] - T_{eest} \right\} \end{aligned} \tag{6}$$

Performing a partial derivation of Eq. (6), the expressions for i_{dest} and i_{qest} can be expressed as

$$\begin{cases} i_{dest} = \frac{2R_f(L_d - L_q)}{3M_{sf}R_s} i_{fest} \\ i_{qest} = \pm\sqrt{\frac{2R_f}{3R_s}\left[1 + \frac{2R_f(L_d - L_q)^2}{3M_{sf}^2 R_s}\right] i_{fest}^2 + \frac{2R_f \psi_{pm}}{3R_s M_{sf}} i_{fest}} \end{cases} \tag{7}$$

where the sign of i_{qest} is determined by the T_{eest} direction, which means that consistent direction is positive, and inconsistent direction is negative.

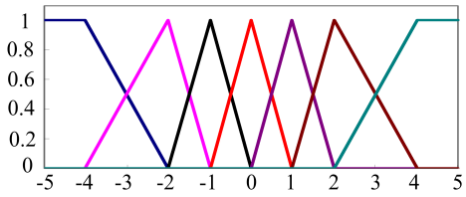

FIGURE 4. The membership functions of ΔE_B and $\Delta\Omega$.

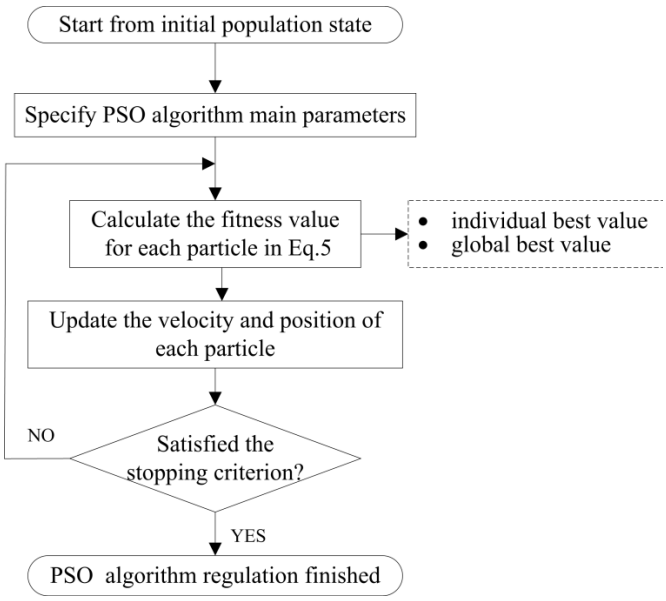

FIGURE 5. Flowchart of the proposed PSO algorithm for flux weakening fuzzy control.

The above expression can be solved by using Newton's iterative method, on the basis of which the estimated current values for i_{dest}, i_{qest} and i_{fest} can be obtained. The above analysis is based on the analysis of HEFMM low-speed region control strategy with minimum copper consumption. When the HEFMM operates at high-speed region than the benchmark speed n_{base}, weak magnetic control needs to be considered to extend the machine operating range, which will be presented in the next section.

3. HEFMM FLUX WEAKENING CONTROL BASED ON FUZZY PSO ALGORITHM

Existing studies have demonstrated that the HEFMM is a complex coupled system with multivariable and strongly nonlinear features. Therefore, due to the variation of M_{sf}, L_d and L_q, the existing control methods do not achieve satisfactory control effect when the HEFMM operates in flux-weakening state.

Fuzzy control algorithm is an intelligent control method with strong logicality and robustness, which is based on fuzzy logic or fuzzy inference system. The obvious merits of this algorithm exist in that the constrained parameter changes easily in linear or nonlinear way without a precise mathematical control model. When HEFMM is operating in the transition state, the incremental fuzzy control method is used to regulate the excitation current and the d-axis current, so that the HEFMM speed enters the stable operation state and improves the dynamic performance of the machine. In order to improve the efficiency of the machine, a particle swarm optimization algorithm is used to further regulate the ratio of the d-axis current and the excitation current after entering the steady state, so as to minimize the machine's copper consumption and to achieve the improvement of the machine efficiency. The estimated q-axis current herein can be calculated from the speed controller. To take full advantage of the terminal voltage and to keep the stability of HEFMM, one current control method that keeps the back electromotive force (back-EMF) almost constant is proposed, that is

$$E_{qest} = \omega_e \left(\psi_{pm} + L_d i_{dest} + M_{sf} i_{fest}\right) = E_{base} \tag{8}$$

$$E_{base} = p\omega_{base}\psi_{pm} \tag{9}$$

where E_{base} and E_{qest} are the base back-EMF and the estimated q-axis back-EMF, respectively.

The principle of the particle swarm algorithm system based on fuzzy theory designed in this paper is shown in Fig. 3, which mainly consists of five parts, i.e., fuzzification, fuzzy rules, fuzzy inference machine, de-fuzzification, and particle swarm optimization controller function module. During the process of flux-weakening speed regulation, in order to ensure the full utilization of the motor to the bus voltage and the stability of the machine operation, the method of keeping the motor counter potential basically unchanged is adopted to regulate the speed. Taking the difference between the estimated counter potential and the base value of counter potential and the speed difference as the input variables of the fuzzy controller, the ΔE_b and Δn expressions can be written as

$$\begin{cases} \Delta E_b = E_{base} - E_{qest} \\ \Delta n = n_{ref} - n_r \end{cases} \tag{10}$$

As shown in Fig. 3, according to the characteristic parameters of the HEFMM prototype, the calibration factors of ΔE_b, Δn, Δi_{dref}, Δi_{fref} are set as $K_{\Delta E_b} = 0.1$, $K_{\Delta n} = 0.02$, $K_{id} = 0.002$, $K_{if} = 0.0015$, and the input variables are calibrated to obtain the corresponding fuzzy variables ΔE_B, ΔN, and the output variables ΔID and ΔIF, which are the precise values of increments of the output variables. According to the fuzzy rules, after fuzzy reasoning, the fuzzy output variables ΔID, ΔIF are obtained, and after calibration, the exact values of the output variable increments $\Delta i'_{dref}$ and $\Delta i'_{fref}$ are obtained. The domains of fuzzy input and output variables

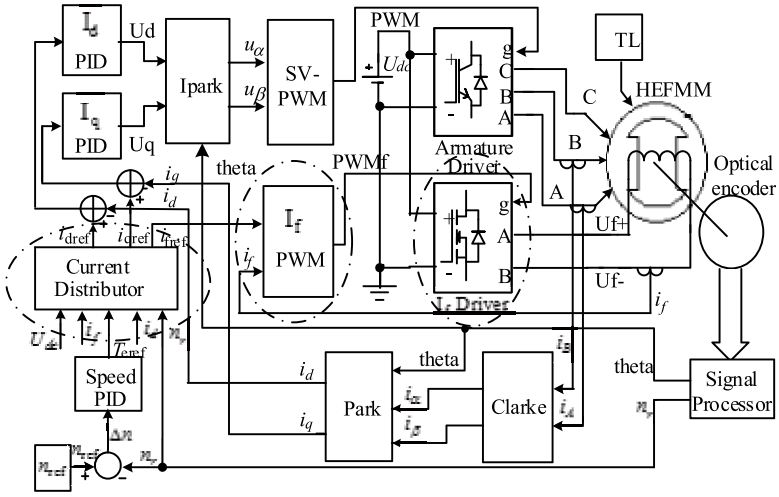

FIGURE 6. Schematic of HEFMM drive system.

are $\{NB, NM, NS, ZO, PS, PM, PB\}$, and the corresponding values are $\{-4, -2, -1, 0, 1, 2, 4\}$. To simplify the calculation, the affiliation functions of ΔE_B and ΔN are distributed in a triangular fashion, as shown in Fig. 4.

With considering the electromagnetic performances of HEFMM, the following four control regulations can be obtained for the setting of fuzzy inference rules, as shown in Table 1.

TABLE 1. Fuzzy rules.

Items	ΔE_b	Δn	i_{fest} and i_{dest}	i_{qest}
Fuzzy R_1	< 0	< 0	$\downarrow$	$\downarrow$
Fuzzy R_2	< 0	> 0	$\downarrow$	$\uparrow$
Fuzzy R_3	> 0	< 0	$\uparrow$	$\downarrow$
Fuzzy R_4	> 0	> 0	$\uparrow$	$\uparrow$

1) When $\Delta E_b < 0$, $\Delta n > 0$, i_{fest} and i_{dest} should be reduced appropriately, meanwhile, the control amount of i_{qest} is increased automatically by speed controller.

2) When $\Delta E_b < 0$, $\Delta n < 0$, i_{fest} and i_{dest} should be decreased appropriately, meanwhile, the control amount of i_{qest}.

3) When $\Delta E_b > 0$, $\Delta n > 0$, i_{fest} and i_{dest} should be increased appropriately, at the same time, the control amount of i_{qest} is increased automatically by the speed controller.

4) When $\Delta E_b > 0$, $\Delta n < 0$, i_{fest} and i_{dest} should be increeased appropriately, and at the same time, the control amount of i_{qest} should be decreased automatically by the speed controller.

In order to realize the good dynamic speed regulation advantage of HEFMM, fuzzy control method is used to regulate the machine speed during its transient process for wide range operation. However, the currents given by the fuzzy control are not the optimal solutions in most of the cases in terms of operating efficiency, and there is a need to find an improved algorithm that skills to optimize the HEFMM current and also keep the machine running stably. For the proposed HEFMM, the PSO algorithm is used to regulate both the d-axis current and the field current according to Eq. (4). The control flowchart of the HEFMM based on the PSO algorithm is shown in Fig. 5.

4. IMPLEMENTATION AND SIMULATION OF HEFMM DRIVE SYSTEM

Figure 6 shows the HEFMM drive control system model. Compared with the typical PMSM and HESM vector control systems, the HEFMM drive control system has three more functional modules, which are the excitation current control signal I_f driver PWM, excitation drive I_f and current allocation module, respectively. For the HEFMM drive control system, the most critical part is the current distribution module, which adopts different current algorithms to coordinate the distribution of armature current and excitation current according to the speed partition, and adopts the conventional copper consumption minimum control in the low-speed region, and adopts the fuzzy weak magnetism control method based on PSO in the high-speed region, in order to realize the stable, reliable, and high-efficiency operation of the machine.

The current distributor is a key module for HEFMM drive control system, as shown in Fig. 7, which is used to regulate field current, d-axis and q-axis currents. The whole speed region is divided into two sub-regions, namely low speed and high speed regions, the conventional MCL control is adopted

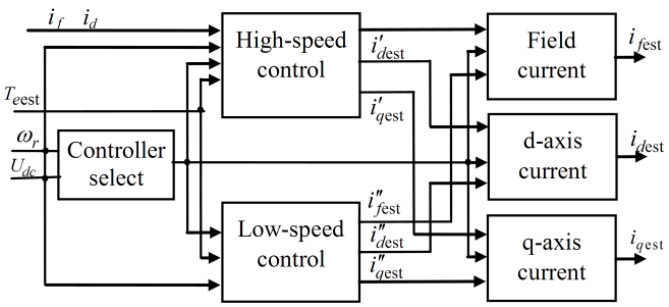

FIGURE 7. HEFMM current distributor.

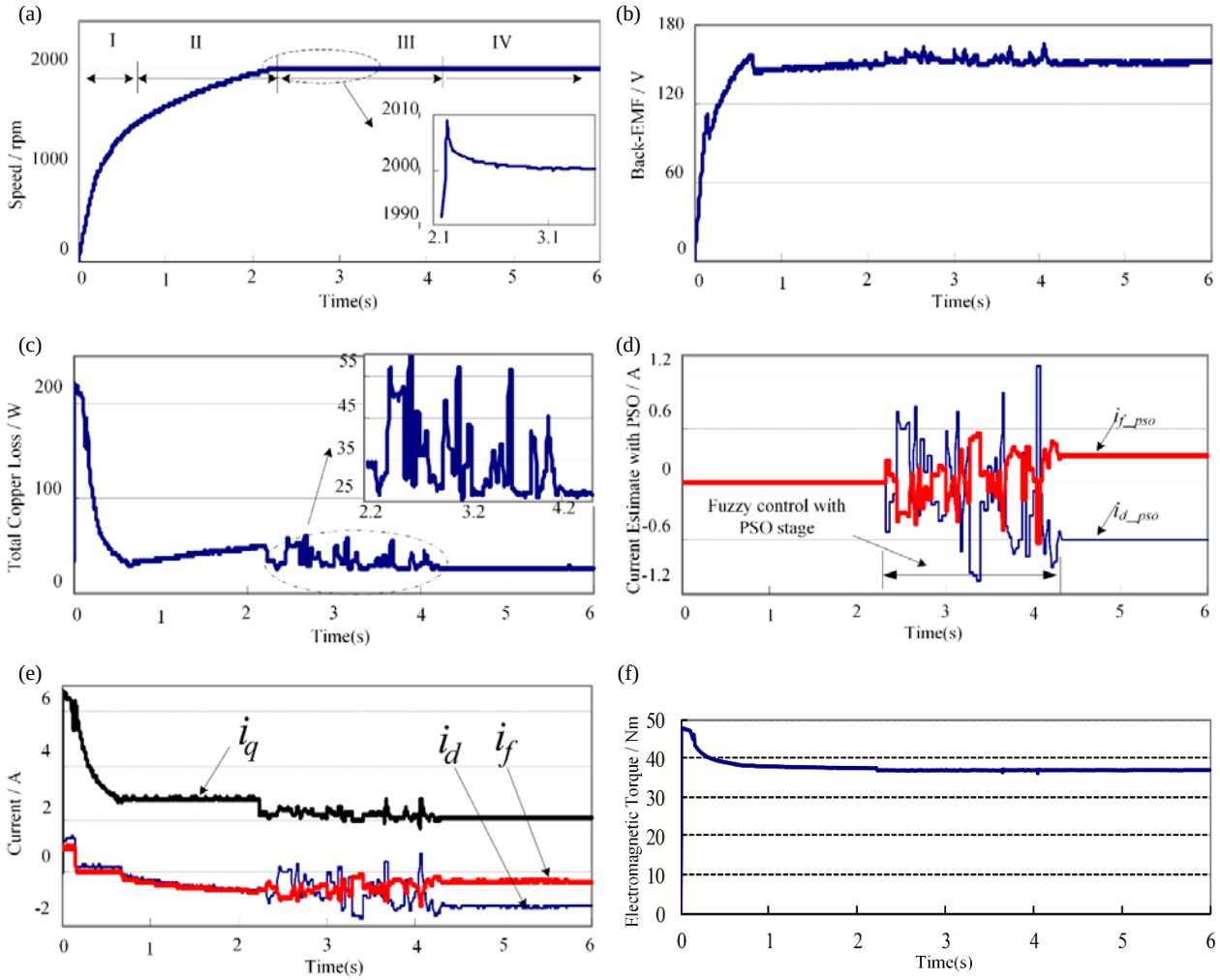

FIGURE 8. The simulation results of HEFMM control system. (a) Startup process speed curve of the HEFMM. (b) Back-EMF waveform. (c) Total copper losses changing waveform. (d) Increments of field current and d-axis current waveforms. (e) Field current, d-axis current, q-axis current waveforms. (f) Torque waveform.

in low speed region and the high speed region is controlled by fuzzy control method combined with PSO algorithm.

In order to verify the effectiveness of the proposed control principles and control model aforementioned, simulations have been carried out for a HEFMM drive system by Simulink. Main parameters of HEFMM are given in Table 2.

Figure 8(a) shows the curve of speed increase during the startup process, and the speed increase has gone through four stages: Part I low-speed zone copper consumption minimization control stage, at this time, the goal is to keep the total copper consumption of the motor at a minimum; Part II fuzzy weak magnetism control stage, this stage relies on the fuzzy rules of the weak magnetism control of the motor; Part III fuzzy control combined with the optimization of PSO algorithm stage, this stage needs to be the combination of fuzzy rules with the optimization of PSO algorithm control parameters; Part IV steady state operation stage after optimization; Part IV optimization is completed; Part IV steady state operation stage after optimization. Fig. 8(b) shows the waveform of the reverse potential, which is basically kept constant in the steady state weak magnetism operation stage, with small fluctuations in the implementation of the PSO optimization stage due to the different inductances of the armature winding and the excitation winding. Fig. 8(c) shows the total copper consumption change waveform of the HESM, the total copper consumption is 32 W when the machine reaches steady state at the end of the startup process, and after three consecutive rotational speed detections with an error of less than 3 rpm, then PSO optimization will be implemented, and during the optimization process, the total copper consumption will fluctuate, and the current value corresponding to the minimum value will be recorded, and after 1.79 seconds, the PSO optimization will be completed using this set of currents as a reference value superimposed to the fuzzy controller output current, at which time the total copper consumption is reduced to 25 W, i.e., 22.8% reduction. Fig. 8(d) shows the waveforms of d-axis current and excitation current component changes obtained using the PSO algorithm, the PSO controller output current is 0 during the motor startup phase, and the PSO optimization is implemented after reaching the steady state, and the optimization process is

Items (symbol)	Value	Unit
Rated power P_N	1000	W
Rated torque T_N	47.6	Nm
PM material	NdFeB	-
B_r	1.1	T
U_{dc}	300	V
R_f	47.1	Ω
R_s	3.86	Ω
L_q	38.6	mH
L_d	54.3	mH
M_{sf}	108.5	mH
I_{fN}	1.0	A
I_N	5	A
Ψ_{pm}	0.35	Wb
L_f	0.57	H

TABLE 2. Main parameters of HEFMM.

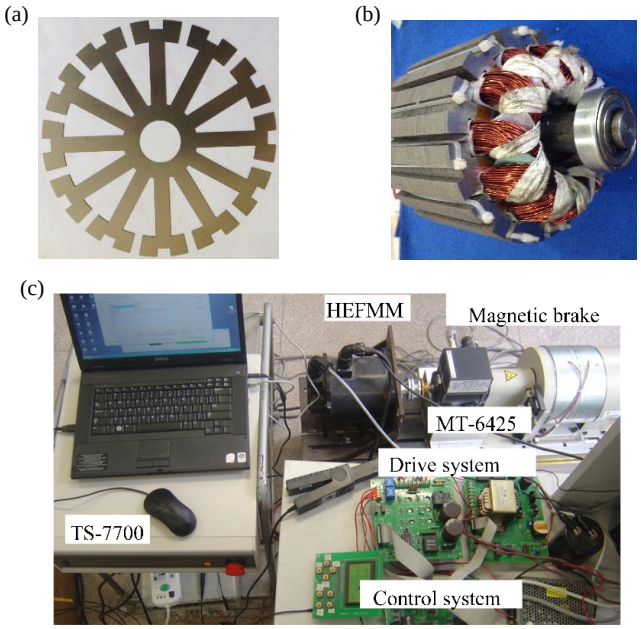

FIGURE 9. Experimental platform for HEFMM. (a) Prototype stator lamination, (b) prototype stator with armature winding, (c) prototype test platform and control system.

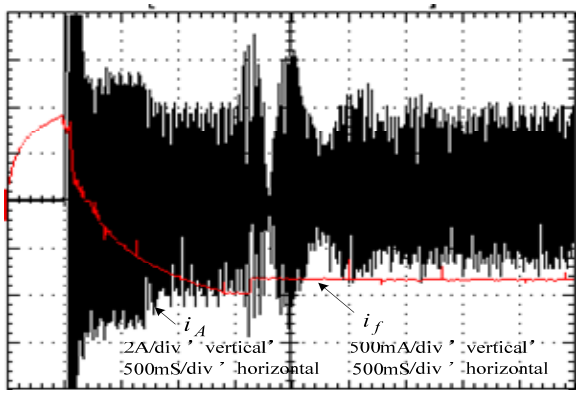

FIGURE 10. Test waveforms of starting current.

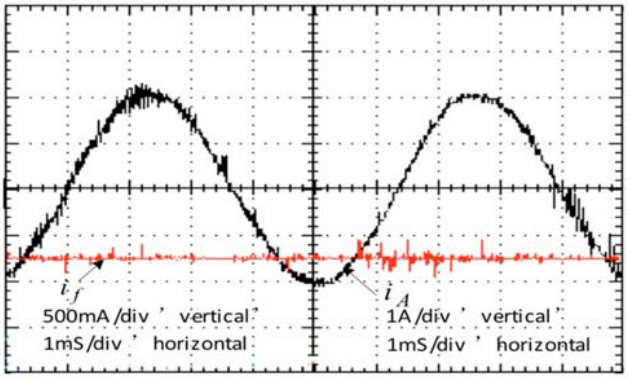

FIGURE 11. HEFMM steady-state current waveforms during flux weakening operation.

maintained at 40 ms for the action time of each group of current values (corresponding to each particle), and each current is applied in turn. Figs. 8(e) and (f) show the measured values of excitation current, d-axis current, q-axis current and electromagnetic torque.

5. EXPERIMENTAL SYSTEM TESTS

One HEFMM prototype is manufactured, as shown in Fig. 9(a) and Fig. 9(b). And its whole test platform is established to verify the correctness of simulation results, which contains five parts, as shown in Fig. 9. HEFMM prototype rated DC bus voltage is 300 V. Fig. 10 shows the HEFMM starting current characteristics. The steady state output torque of the motor is 47.6 Nm, and according to the definition of torque density, the torque density of the HEFMM motor can be obtained as 16.2 kNm/m^3, which is much higher than the torque density of the conventional PMSM with the radial PM arrangement.

In order to enhance the starting torque capacity of the proposed HEFMM, considering the large inductance value of the excitation winding of the HEFMM, in order to improve the starting torque capability of the proposed HEFMM, a positive rated excitation current is applied to the machine for half a second before starting the armature current. As this current value increases, the HEFMM speed decreases gradually accordingly. When HEFMM speed exceeds the base speed, the speed governing weak magnetic control is started.

Figure 11 indicates the HEFMM steady-state current waveform, which demonstrates a high sinusoidal degree, implying a low harmonic component.

6. CONCLUSION

Based on adding hybrid excitation principle into the magnetic field modulation machine, a new type of HEFMM is proposed and designed in this paper. In order to improve the dynamic response of the proposed machine and reduce the impact of machine parameter changes on its control performance, an intelligent control strategy combining fuzzy control and PSO optimization algorithm is designed and implemented. According to the magnetic field adjusting property, the whole operation region is divided into two speed regions, and MCL control and flux weakening fuzzy control with PSO algorithm are employed for the two regions for the HEFMM, respectively. Both simulation and experimental results verify the validity of the proposed machine performance, and the following conclusions could be drawn:

(1) The proposed control system is a partitioned control system based on rotor magnetic field orientation, and different control strategies are applied to different speed ranges according to the electrical characteristics of HEFMM. The experiment shows that the HEFMM control system can stably and smoothly switch between different speed ranges.

(2) During the low-speed and high-speed areas, a magnetic regulation method combining excitation current and d-axis current is adopted. Compared with the existing HEFMM control system that only uses excitation current magnetic regulation for speed regulation, it has significant low-speed, high torque, and wide speed regulation characteristics.

(3) During the process of weak magnetic speed regulation in high-speed areas, the decoupling control of d-axis current and excitation current is effectively achieved by keeping the back electromotive force unchanged and adjusting them in zones, simplifying the control algorithm of HEFMM. The simulation results show that this current optimization method can effectively reduce the total copper loss of the machine by 22.8%, achieving the efficiency optimization of this type of machine control.

(4) AHEFMM prototype with one kilowatt rated power is designed and the corresponding characteristics are tested. The experimental results show that the proposed machine has good dynamic field weakening speed regulation capacity, which has a good application prospect in the field of low-speed direct drive for EVs. Both simulation and experimental results verify that the total copper losses are decreased significantly and the operation range of speed regulation is broadened with higher efficiency by using PSO algorithm.

ACKNOWLEDGEMENT

This work was supported by Scientific and Technological Program of Henan Science and Technology Agency (212102210022, 232102220065), Key Innovation Projects for University Students (202311517009), Key Research Projects of Higher Education Institutions in Henan Province (24A470002, 24B510001), Ministry of Education Collaborative Education Program (230702910213146) and the Scientific Research and Cultivation Foundation of Henan University of Engineering (D2022012).

REFERENCES

[1] Yang, C., H. Lin, H. Guo, and Z. Q. Zhu, "Design and analysis of a novel hybrid excitation synchronous machine with asymmetrically stagger permanent magnet," *IEEE Transactions on Magnetics*, Vol. 44, No. 11, 4353–4356, Nov. 2008.

[2] Zhang, Y., J. Luo, M. Huang, Q. Huang, and D. Decker, "Design and experimental verification of variable flux permanent magnet vernier machine using time-stepping finite element method," *Progress In Electromagnetics Research C*, Vol. 129, 115–126, 2023.

[3] Zhang, Y., Q. Huang, M. Huang, D. Decker, and Y. Qing, "Design and experimental verification of adaptive speed region control for hybrid excitation claw-pole synchronous machine," *Progress In Electromagnetics Research C*, Vol. 88, 195–205, 2018.

[4] Cai, S., Z.-Q. Zhu, C. Wang, J.-C. Mipo, and S. Personnaz, "A novel fractional slot non-overlapping winding hybrid excited machine with consequent-pole pm rotor," *IEEE Transactions on Energy Conversion*, Vol. 35, No. 3, 1628–1637, Sep. 2020.

[5] Fan, Y., Y. Lei, and X. Wang, "An improved robust deadbeat predictive current control for the consequent-pole hybrid excitation motor," *IEEE Transactions on Energy Conversion*, Vol. 38, No. 2, 1219–1230, Jun. 2023.

[6] Wang, S., S. Niu, and W. Fu, "Comparative study of relieving-dc-saturation hybrid excited vernier machine with different rotor pole designs for wind power generation," *IEEE Access*, Vol. 8, 198 900–198 911, Sep. 2020.

[7] Zhang, Z., Y. Liu, B. Tian, and W. Wang, "Investigation and implementation of a new hybrid excitation synchronous machine drive system," *IET Electric Power Applications*, Vol. 11, No. 4, 487–494, Apr. 2017.

[8] Jian, L., G. Xu, Y. Gong, J. Song, J. Liang, and M. Chang, "Electromagnetic design and analysis of a novel magnetic-gear-integrated wind power generator using time-stepping finite element method," *Progress In Electromagnetics Research*, Vol. 113, 351–367, 2011.

[9] Cheng, M., P. Han, and W. Hua, "General airgap field modulation theory for electrical machines," *IEEE Transactions on Industrial Electronics*, Vol. 64, No. 8, 6063–6074, Mar. 2017.

[10] Yu, Z., W. Kong, R. Qu, D. Li, S. Jia, D. Jiang, J. Sun, and H. Li, "Optimal three-dimensional current computation flux weakening control strategy for dc-biased vernier reluctance machines considering inductance nonlinearity," *IEEE Transactions on Power Electronics*, Vol. 34, No. 2, 1560–1571, Feb. 2019.

[11] Zhu, Z. Q. and D. Evans, "Overview of recent advances in innovative electrical machines-with particular reference to magnetically geared switched flux machines," in *2014 17th International Conference on Electrical Machines and Systems (ICEMS)*, 1–10, Oct. 2014.

[12] Zhao, X., S. Niu, X. Zhang, and W. Fu, "A new relieving-dc-saturation hybrid excitation vernier machine for hev starter generator application," *IEEE Transactions on Industrial Electronics*, Vol. 67, No. 8, 6342–6353, Aug. 2020.

[13] Liu, C., K. T. Chau, J. Z. Jiang, and L. Jian, "Design of a new outer-rotor permanent magnet hybrid machine for wind power generation," *IEEE Transactions on Magnetics*, Vol. 44, No. 6, 1494–1497, Jun. 2008.

[14] Yang, H., H. Lin, Z. Q. Zhu, S. Fang, and Y. Huang, "Novel flux-regulatable dual-magnet vernier memory machines for electric vehicle propulsion," *IEEE Transactions on Applied Superconductivity*, Vol. 24, No. 5, 1–5, Oct. 2014.

[15] Hua, H. and Z. Q. Zhu, "Comparative study of series and parallel hybrid excited machines," *IEEE Transactions on Energy Conversion*, Vol. 35, No. 3, 1705–1714, Sep. 2020.

[16] Deng, Y. W., K. Wang, J. Li, and T. Wang, "Comparison of different flux-weakening strategies of ac-excited hybrid excitation synchronous motor," in *2022 25th International Conference on Electrical Machines and Systems (ICEMS)*, 1–5, Nov./Dec. 2022.

[17] Daniel, M., Y. Yokoi, and T. Higuchi, "A comparative study of hybrid excited half-wave rectified synchronous motor with different hybridization ratios considering electric vehicle operating conditions," in *2021 24th International Conference on Electrical Machines and Systems (ICEMS 2021)*, 432–436, Gyeongju, South Korea, Oct. 2021.

[18] Cinti, L., P. G. Carlet, L. Ortombina, and N. Bianchi, "Flux-weakening control of hybrid-excited permanent magnet synchronous motors," in *2022 IEEE Energy Conversion Congress and Exposition (ECCE)*, 1–8, Detroit, MI, Oct. 2022.

[19] Ostroverkhov, M., Y. Monakhov, and V. Chumack, "Study of robust speed control of hybrid excited synchronous machine with field weakening," in *IEEE Problems of Automated Electrodrive Theory and Practice*, 1–5, Sep. 2020.

[20] Huang, M., H. Lin, H. Yunkai, P. Jin, and Y. Guo, "Fuzzy control for flux weakening of hybrid exciting synchronous motor based on particle swarm optimization algorithm," *IEEE Transactions on Magnetics*, Vol. 48, No. 11, 2989–2992, Nov. 2012.

[21] Zhao, J., M. Lin, D. Xu, L. Hao, and W. Zhang, "Vector control of a hybrid axial field flux-switching permanent magnet machine based on particle swarm optimization," *IEEE Transactions on Magnetics*, Vol. 51, No. 11, 1–4, Nov. 2015.

[22] Jia, S., R. Qu, W. Kong, D. Li, J. Li, Z. Yu, and H. Fang, "Hybrid excitation stator PM vernier machines with novel dc-biased sinusoidal armature current," *IEEE Transactions on Industry Applications*, Vol. 54, No. 2, 1339–1348, Mar. 2018.